**Toxicology International,** *31(4) : 579-592; 2024. DOI: 10.18311/ti/2024/v31i4/43048*

Online ISSN : 0976-5131; Print ISSN : 0971-6580

Toxicology International

Contents available at: www.informaticsjournals.co.in/index.php/toxi




# Characterization of Stress Degradation Products of Asenapine by LC-MS/MS and Elucidation of their Degradation Pathway

**Doppala Madhu[1], Sireesha Koneru[2], Bhagya Kumar Tatavarti[3], Kandula Rekha[4] and Venkateswara Rao Anna[1*]**

*[1]Department of Chemistry, Koneru Lakshmaiah Education Foundation, Vaddeswaram, Guntur - 522302, Andhra Pradesh, India; avrchemistry@gmail.com*

*[2]Department of Mechanical Engineering, Koneru Lakshmaiah Education Foundation, Vaddeswaram, Guntur - 522302, Andhra Pradesh, India*

*[3]Department of Chemistry, K.B.N. College (Autonomous), Kothapeta, Vijayawada - 520001, Andhra Pradesh, India*

*[4]Department of Biotechnology, Dr.V.S Krishna Government Degree College, Visakhapatnam - 530022, Andhra Pradesh, India*

## Abstract

The investigation aimed to integrate Liquid Chromatography (LC) and Liquid Chromatography-Mass Spectrometry (LC–MS) for precise separation, identification, and characterization of asenapine's Degradation Products (DPs) without isolating them from reaction mixtures. Asenapine underwent scrutiny under various stress conditions (oxidative, hydrolytic, thermal, and photolytic) following ICH Q1A(R2) guidelines. A total of five distinct degradation products emerged from these stress conditions. The separation of all degradation products was executed utilizing a BDS Y Persil C18 column employing with 0.1 % orthophosphoric acid, acetonitrile, and methanol in the ratio of 50:30:20 (v/v) as mobile phase as an isocratic mode with 231 nm. Elucidation of these degradation products was achieved by scrutinizing their fragmentation pattern and the masses discerned through LC–MS/MS and $MS^n$ analysis. These previously unidentified degradation products were ascertained to be 11-chloro-3a,12b-dihydro-1H-dibenzo[2,3:6,7] oxepino[4,5-c]pyrrole (DP 1), 3-(3-chloro-6-methylidenecyclohexa-2,4-dien-1-yl)-4-(cyclohexa-1,4-dien-1-yl)-1-methylpyrrolidine (DP-2), 5-chloro-2-methyl-2,3,3a,12b-tetrahydro-1H-dibenzo[2,3:6,7]oxepino[4,5-c]pyrrole 2-oxide (DP 3), 2-(1-methyl-4-phenylpyrrolidin-3-yl)cyclohexa-2,5-dien-1-ol (DP-4) and 13-(cyclohexa-1,3-dien-1-yl)-1-methyl-4-(6-methylidenecyclohexa-1,4-dien-1-yl)pyrrolidine (DP-5). Based in findings, it was confirmed that the method was appropriate for resolution, identification and quantification of impurity 1 and 2 of asenapine along with its DPs.

**Keywords:** Asenapine, Antipsychotic Drug, Bipolar Disorder, Degradation Products (DPs)

**Author for correspondence*

Article Received on: 25.03.2024 Revised on: 16.08.2024 Accepted on: 13.09.2024

## 1. Introduction

Antipsychotic drugs, alternatively referred to as neuroleptics, are medications primarily employed in the treatment of psychosis symptoms, encompassing hallucinations, delusions, disorganized thinking, and agitation[1]. These medications are frequently prescribed for the management of psychiatric conditions like schizophrenia, bipolar disorder, and severe depression accompanied by psychotic symptoms. These medications function by regulating neurotransmitter activity within the brain, notably targeting dopamine and serotonin. These neurotransmitters play crucial roles in governing mood, cognition, and perception[2,3]. Antipsychotic drugs are primarily utilized manage symptoms associated with psychosis, including delusions, hallucinations, disorganized thinking and speech, and agitation[4]. It's important to note that antipsychotic medications should be used judiciously, with close monitoring by a healthcare professional, due to the potential for side effects such as weight gain, metabolic changes, sedation, and movement disorders[5].

Stress degradation impurities refer to the byproducts or degradation products that form when a pharmaceutical drug substance or product is subjected to various stress conditions during manufacturing, storage, or testing. These stress conditions can include exposure to heat, humidity, light, acid and base hydrolysis, oxidation, and other chemical or physical factors[6]. stress impurity analysis is critical for ensuring the efficacy, safety, and quality of pharmaceutical products, as well as compliance with regulatory standards. It facilitates on-going quality control, process optimization, and risk assessment throughout the drug development and manufacturing lifecycle[7].

Impurity analysis using HPLC is essential throughout the drug development process, from early-stage research to quality control in manufacturing. HPLC is indispensable for impurity analysis in drugs, providing pharmaceutical scientists with valuable insights into the composition and quality of pharmaceutical products, ultimately ensuring the safety and efficacy of medications for patients. HPLC is invaluable for impurity analysis and the identification of degradation pathways in pharmaceuticals. It enables the separation, quantification, and identification of impurities, as well as structural determination of DPs formed under various stress conditions. This information is essential for ensuring the quality, safety, and efficacy of pharmaceutical products throughout their lifecycle[8,9].

Asenapine is a medication primarily used to treat schizophrenia and bipolar disorder. It belongs to the class of atypical antipsychotic drugs, which work by altering the effects of certain chemicals in the brain. Asenapine is unique in that it is administered sublingually, meaning it is absorbed through the tissues under the tongue[10]. Effectiveness in alleviating symptoms such as hallucinations, delusions, mood swings, and other psychotic manifestations linked to schizophrenia and bipolar disorder[11]. Very common side effects of asenapine may include dizziness, dry mouth, weight gain and drowsiness[12]. Molecular formula of asenapine (Figure 1) is $C_{17}H_{16}CINO$: $C_4H_4O_4$ with 401.84 g/mol as molecular mass and (3aR,12bR)-5-Chloro-2-methyl-2,3,3a,12b-tetrahydro-1H-dibenzo [2,3:6,7] oxepino[4,5-c] pyrrole maleate.

In literature survey of asenapine estimation by using HPLC in pharmaceutical formulation[13-20], UV and HPLC estimation in dosage of tablets[21], asenapine in dissolution media and *in-vitro* release from co-crystals[22], lipidic nano formulations of asenapine[23], hair and nail clippings[24], combination asenapine with valproic acid of simultaneous determination in human plasma by LC-MS[25], inactive metabolites in human plasma by LC-MS/MS[26], and solid-phase extraction and metabolites estimation by LC-MS[27], there is gap of asenapine and its degradation products and its characterization. The present study is aimed to explain about degradation products of asenapine by LC–MS/MS analysis along with its impurities. In Figure 2 represents details of impurities.

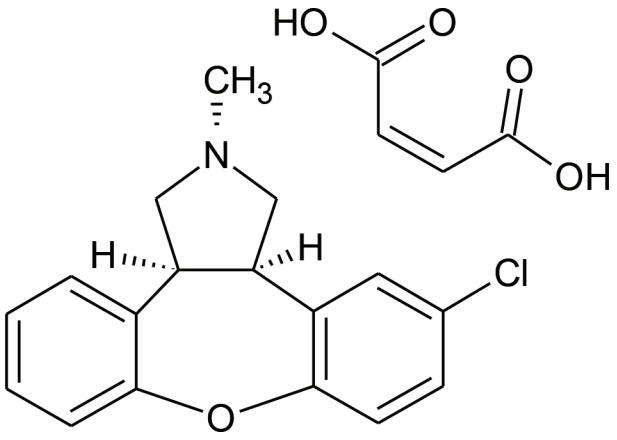
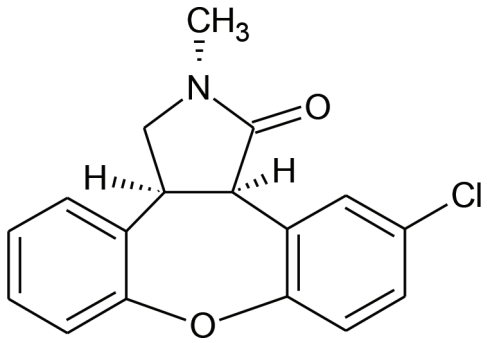
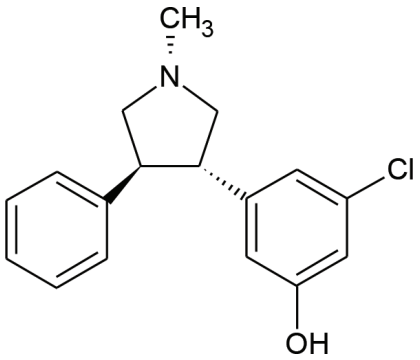



**Figure 1.** Structure of asenapine.




**Impurity 1**
**Molecular formula:** $C_{17}H_{16}CINO_2$
**Molar mass:** 299.75 g/mol
**IUPAC Name:** (3aS,12bS)-11-chloro-2-methyl-2,3,3a,12b-tetrahydro-1H-dibenzo [2,3:6,7] oxepino[4,5-c] pyrrol-1-one




**Impurity 2**
**Molecular formula:** $C_{17}H_{18}CINO$
**Molar mass:** 287.78 g/mol
**IUPAC Name:** Trans-N-methyl-3- (2-hydroxy-5-chlorophenyl)-4- phenyl-pyrrolidine hydrobromide

**Figure 2.** Systemic details of asenapine impurities in this study.

# 2. Experimental

## 2.1 Reagents and Drugs

Asenapine (API) with 99.5% purity along with impurities were achieved from Ryon pharma,

Ludhiana, Punjab. Solvents like methanol, acetonitrile, water and buffer solutions with HPLC grade was purchased from Merck chemicals, Mumbai. We obtained analytical reagent grade hydrochloric acid (HCl) from Qualigens Fine Chemicals Pvt. Ltd. (Mumbai, India) and 30% hydrogen peroxide from S.D. Fine-Chem. Ltd. (Mumbai, India). Asevator (10mg) formulation was obtained from local pharmacy.

## 2.2 Equipments

LC analysis was conducted using a HPLC system (1200 Infinity series, Agilent Technologies, USA), comprising a gradient quaternary pump, auto-sampler, UV detector, and chem station software. Mass experiments were carried out on a waters LC-MS/MS system (waters, USA), featuring a binary solvent delivery pump, autosampler, triple-quad mass detector, and mass lynx software. The pH of the mobile phase was measured using a systronics pH meter (India).

## 2.3 Forced Degradation

The objective was to achieve 10%–15% degradation of the asenapine in forced degradation studies. Asenapine was tested under different stresses: Oxidation, hydrolysis, heat, and light. Results were compared among four samples for each condition, untreated blank, stressed blank, untreated standard drug, and stressed drug solution.

### *2.3.1 Hydrolytic Degradation*

1 ml of asenapine stock solution (1000 µg/ml) was mix with 1 ml of HCl (1 M) and NaOH (1 M) in a 10 ml volumetric flask and was heated at 80°C for 24 h. Before injection into the LC-MS/MS system, samples were neutralized using an equivalent amount of acid or alkali.

### *2.3.2 Oxidative Degradation*

Oxidative degradation utilized hydrogen peroxide. 1 ml of 1000 µg/ml asenapine solution mixed with 1 ml of 30% hydrogen peroxide in a 10 ml flask and heated at 80°C for 24 h. After exposure, samples were diluted to volume with diluent and analysed by LC-MS/MS.

### *2.3.3 Thermal Degradation*

10 mg of the drug samples were individually placed in 10 ml volumetric flasks and sealed. One flask underwent dry heat treatment in a hot air oven at specific temperature and time intervals, while the other flask remained untreated as the control. Following exposure, solutions were prepared by weighing the appropriate amounts of the thermally stressed sample and the control to reach a concentration of 100 µg/ml. These solutions were then diluted to volume using a diluent and separately injected into the LC-MS/MS system.

### 2.3.4 Photodegradation

A 1mm drug layer was prepared for photostability testing under ICH conditions and compared with a control sample, both subsequently diluted and analysed using LC-MS/MS. Two 100µg/ml drug solutions were prepared in 10ml volumetric flasks using methanol, with one subjected to ICH recommended light exposure for photodegradation studies and the other maintained as a control.

## 2.4 Method Development

The process of separating the standard compound from its impurities involved a series of trials to find the most effective conditions. This included experimenting with different solvents as mobile phases and varying flow rates. The aim was to achieve optimal separation of the standard compound and its impurities on the chromatographic column. During these trials, various combinations of solvents such as acetonitrile, methanol, and water were tested, each with different proportions. Additionally, adjustments were made to the pH of the buffer used in the mobile phase to further optimize the separation process. The goal was to find a combination of solvents and buffer pH that would provide the best resolution and peak shape, allowing for accurate quantification of both the standard compound and its impurities. This process required careful experimentation and analysis to identify the conditions that yielded the most satisfactory separation. By systematically adjusting the mobile phase composition and flow rates, the separation method could be fine-tuned to ensure efficient and reliable analysis. This iterative process is essential in chromatographic method development to achieve the desired separation and analytical performance. Various trails were conducted for the separation of standard and impurities. The separation was performed by using different solvents as mobile phase, and different flow rates. The separation was achieved by adjusting the proportions of acetonitrile, methanol, water and, while altering the buffer's pH.

## 2.5 Method Validation

The LC method was validated in accordance with the ICH guidelines Q2(R1)[28], encompassing a range of parameters. These included assessing linearity, precision (both inter-day and intra-day), accuracy, specificity, and selectivity.

### 2.5.1 Linearity

The method's linearity was confirmed by employing solutions with drug of different concentrations. Each sample demonstrating linearity was injected into the HPLC column in triplicate, maintaining a constant injection volume.

### 2.5.2 Precision

Precision analysis involved injecting the drug at three different concentrations (50%, 100%, and 150%) in triplicate into the HPLC system on consecutive days. Standard deviation and % RSD were calculated to assess both intra-day and inter-day precision.

### 2.5.3 Accuracy

The method's accuracy was confirmed via recovery studies, wherein the pure drug was retrieved from degraded samples using the standard addition technique. Stressed sample blends were augmented with the drug at different concentrations.

### 2.5.4 Robustness

Robustness assessment involved meticulous adjustments to parameters such as temperature, mobile phase pH, and other relevant factors, with intentional minor modifications encompassing both positive and negative variations in detector wavelength (within ±5 nm), flow rate (within ±0.05 mL/min), and column oven temperature (with ±3°C alteration). Tabulation of % area response change and system suitability data was conducted to ensure method robustness.

### 2.5.5 Specificity and Selectivity

The specificity of the method was evaluated by calculating the resolution factor between the drug peak and its closest resolving peak, as well as with other peaks present. Selectivity was confirmed through peak purity studies using a detector. To achieve this, a mixture of degradants was prepared by combining equal volumes of solutions generated under different stress conditions, followed by analysis using HPLC

### 2.5.6 Sensitivity

The LOD and LOQ of impurities in this method were established to ensure method sensitivity adherence. The minimum analyte concentration detectable and

quantifiable in the matrix by the instrument was defined as LOD and LOQ, respectively. Consistency in LOD concentration was expected across accuracy, precision, and linearity ranges upon each injection, without variation.

### 2.6 Mass Spectral Studies

Mass spectral analyses were conducted using positive Electrospray Ionization (ESI) mode over a mass range of 0–500 Da to elucidate the drug's fragmentation pattern. Measures were taken to ensure clear mass spectra free of background noise. The mass parameters were finely adjusted to obtain a distinct molecular ion peak of the drug, utilizing high purity nitrogen as both the nebulizer and auxiliary gas, followed by subsequent MS/MS analysis in positive ESI mode to investigate the origin of each individual fragment.

### 2.7 LC-MS/MS Studies

Degraded drug samples underwent LC-MS/MS analysis in positive ESI mode employing a previously established gradient LC method, resulting in successful separation of degradation products utilizing a C18 column. Samples exhibiting maximum degradation were selected for LC–MS analysis to elucidate the structural identity of each degradation product through fragmentation analysis[29-32].

## 3. Results and Discussion

### 3.1 Degradation Behaviour

The chromatogram shown in Figure 2 displays the degradation pattern of asenapine, producing five byproducts labeled 1-5. The primary byproduct, DP-1, emerged under acidic and basic conditions, while DP-3 appeared only in an oxidative degradation. DP-4 were minor byproducts formed exclusively under acid conditions, DP- 2 and 5 were formed under base degradation, underscoring asenapine's sensitivity to base and prompting the need for manufacturers to minimize NaOH exposure during production. Conversely, the drug showed stability under oxidative, photo and thermal conditions.

#### *3.1.1 Fragmentation Pathway of Asenapine*

Figure 6 shows that the asenapine total 8 numbers of breaks down into 8 different pieces. The starting

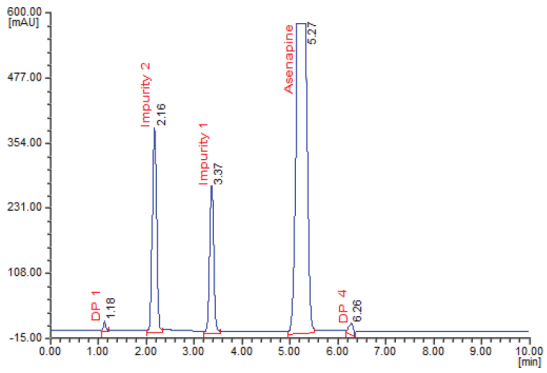



**Figure 3.** Chromaotgram observed in acid stress study of asenapine.

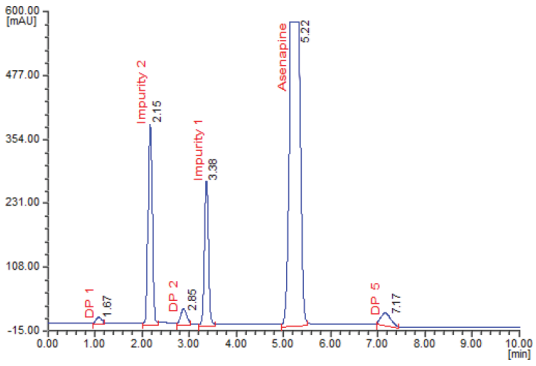



**Figure 4.** Chromaotgram observed in base stress study of asenapine.

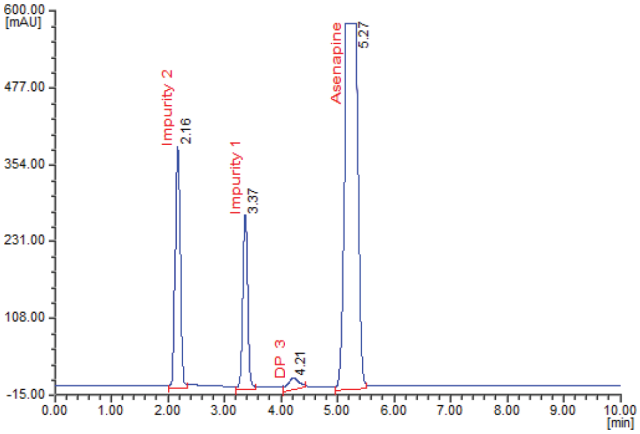



**Figure 5.** Chromaotgram observed in peroxide stress study of asenapine.

molecule of the asenapine, called the molecular ion and has a mass of 285.76. It breaks down in two main ways.

In Figure 7, We see that losing the link of 2-ethylphenol ring and removing a 1-methylpyrrolidine ring creates

fragments with masses of 255.7 and 192.6, respectively. There are two types of break-down products: Those that come from the 2-ethylphenol ring and those that come from the cyclic (ring-like) structure. The fragment with a mass of 156.20 can loss C-Cl bond, and from that again loss of 1-methylpyrrolidine ring to form a smaller ion of 103.14, which then can turn into a ring structure with a mass of 103.14. Meanwhile, the fragment with mass 255.71 forms when a C-C and C-N group is lost from the asenapine standard drug. It can further break down by losing C=C and C-Cl groups from the side chain to form fragments with mass of 207.24. And another fragment was formed by the loss of benzene ring, with mass of 128.17. Lastly, the piece with a mass of 91.12 can lose a vinylacetylene group from its side chain, resulting in an ion with mass 91.12. This process helps us understand how the drug breaks into smaller pieces.

Interpretation data of asenapine is given Table 1.

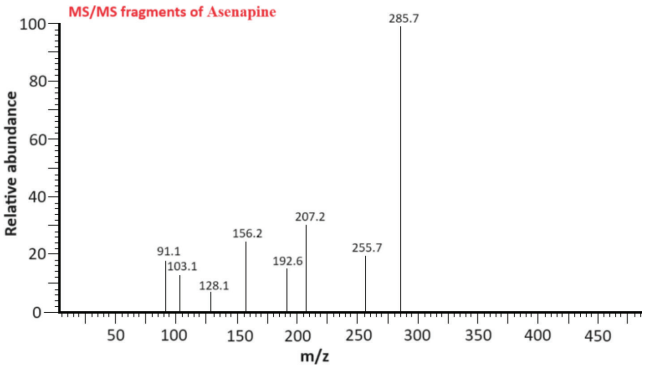



**Figure 6.** Line spectrum of asenapine obtained in MS study.

### 3.1.2 *LC–MS/MS Studies on Forced Degradation Sample*

Five degradation products was formed during the forced degradation study they named as DP 1-5. Mass spectra of degradation products was given in the Figure 8.

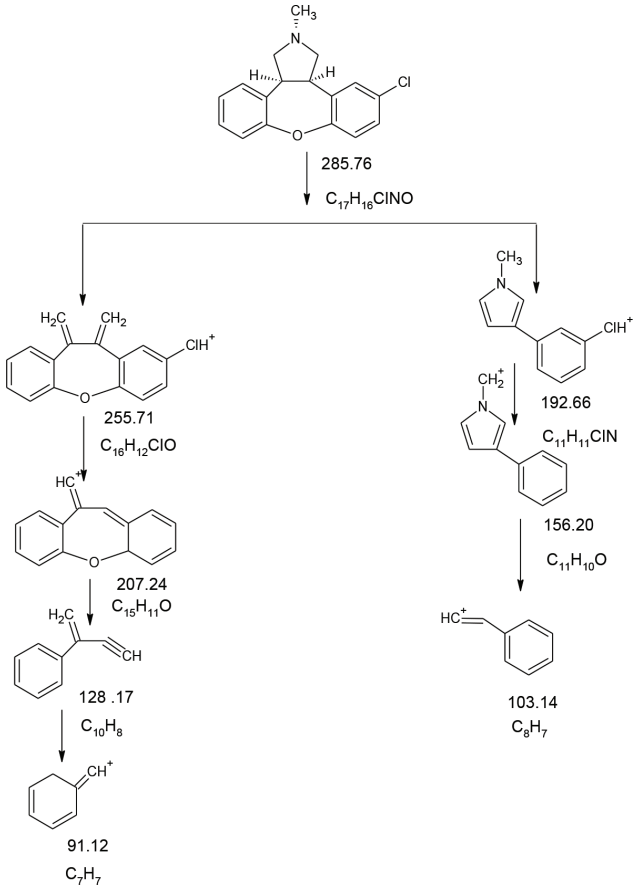
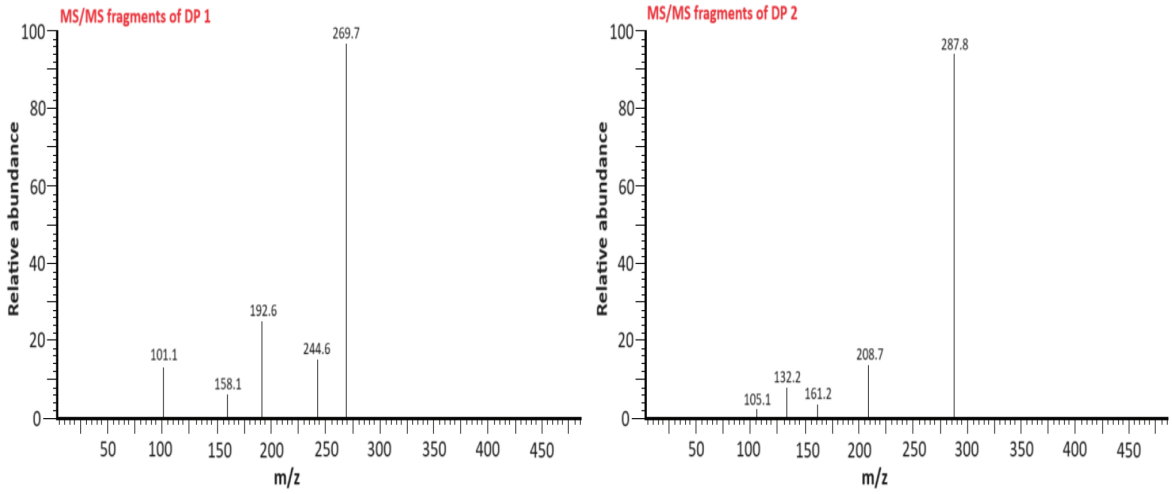



**Figure 7.** Fragmentation pathway of asenapine.

**Table 1.** MS/MS data fragments Interpretation of asenapine

| Peak No. | Observed Molecular Mass | Possible Formula | Calculated Mass | DB* | Difference from Parent Ion | Possible Losses Corresponding to Difference |
|---|---|---|---|---|---|---|
| 0 | 285.34 | $C_{17}H_{16}ClNO$ | 285.76 | 6 | --- | --- |
| 1 | 255.56 | $C_{16}H_{12}ClO$ | 255.71 | 8 | 30.05 | $CH_4N$ |
| 2 | 207.11 | $C_{15}H_{11}O$ | 207.24 | 7 | 48.47 | CHCl |
| 3 | 192.46 | $C_{11}H_{11}ClN$ | 192.66 | 5 | 93.10 | $C_6H_5O$ |
| 4 | 156.13 | $C_{11}H_{10}O$ | 156.20 | 5 | 36.46 | HCl |
| 5 | 128.21 | $C_{10}H_8$ | 128.17 | 4 | 79.07 | $C_5H_3O$ |
| 6 | 103.02 | $C_8H_7$ | 103.14 | 4 | 53.06 | $C_3H_3N$ |
| 7 | 91.09 | $C_7H_7$ | 91.12 | 3 | 37.05 | $C_3H$ |

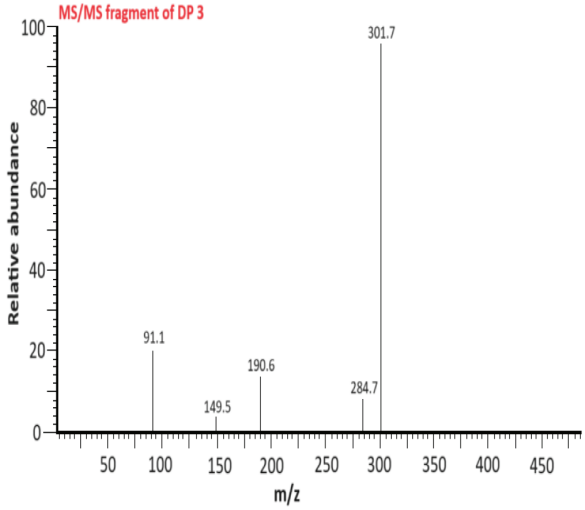
* DB: double bonds



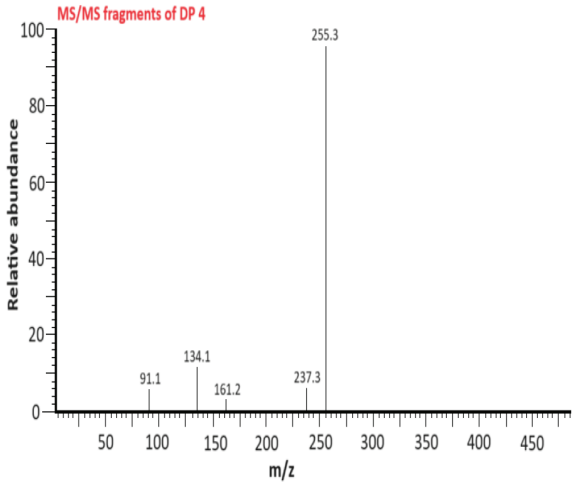

(A) DP 1



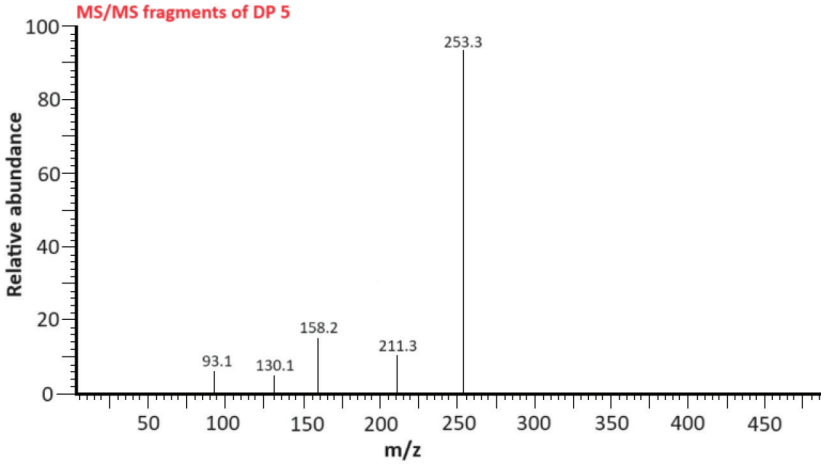

(B) DP 2




(C) DP 3




(D) DP 4




(E) DP 5

**Figure 8.** LC-MS/MS studies of degradation products.

LC–MS/MS data for Degradation Products (DPs) 1-5, accompanied by their probable molecular formulas and prominent fragment ions were given in Table 2.

### *3.1.3 Identification of Degradation Products*

The degradation products were identified by comparing their LC-MS/MS fragmentation patterns with those of the asenapine from MS/MS and $MS^n$ analyses.

**DP 1 (m/z 269.72):**

The fragmentation pathway of DP-1, shown in Figure 9, mass spectrum and further detailed in Figure 8 (A), indicates the DP 1 with molecular mass of m/z 287.35 Initial positive ESI LC-MS analysis yielded four fragments of DP-1 (m/z 244.69, 192.62, 158.17 and 101.12). First product ion from DP 1 is formed due to the loss of $C_2H$ with mass of 244.69 m/z from parent ion, from first product ion another fragment was formed during the loss of $C_4H_4$ with molecular mass of 192.62 m/z. From second product ion by loss of HCl with molecular mass of 158.17 m/z. From product ion of 158.17 another product ion is formed due to the loss of $C_2H_3NO$ with the molecular mass of 101.12 m/z. Hence from all DP 1 was identified as *11*-chloro-3a,12b-dihydro-1H-dibenzo[2,3:6,7]oxepino[4,5-c]pyrrole.

**DP 2 (m/z 287.82):**

DP 2 fragmentation pathway is shown in Figure 9 and mass spectrum shown in Figure 8 (B). In DP 2 parent ion fragment was observed at mass of 287.82 m/z. From that parent ion four product ions are formed. DP 2 product ions showed at 208.70 m/z, 161.70 m/z, 132.20 m/z, and 105.15 m/z. In addition, 208.70 m/z characteristic product ion formed due to the loss of $C_6H_7$ (1,3-Cyclohexadienylium). Alternately 161.70 m/z was formed from 208.70 m/z due to the loss of CCl. From product ion of 161.70 m/z, 132.20 m/z product ion was formed due to the loss of $CH_3N$ (Methanimine), and finally from this last by product ion was formed due to the loss of $C_2H_3$ (Ethenyl) with mass of 105.15 m/z. Finally, DP 2 was identified as 3-(3-chloro-6-methylidenecyclohexa-2,4-dien-1-yl)-4-(cyclohexa-1,4-dien-1-yl)-1-methylpyrrolidine.

**DP 3 (m/z 301.76):**

The fragmentation pathway of DP-3, shown in Figure 9, mass spectrum and further detailed in Figure 8 (C), indicates the DP 3 with molecular mass of m/z 301.76. Initial positive ESI LC-MS analysis yielded four fragments of DP-3 (m/z 284.75, 190.64, 149.59 and 91.12). First product ion from DP 3 is formed due to the loss of HO with mass of 284.75 m/z from parent ion, from first product ion another fragment was formed during the loss of $C_6H_6O$ with molecular mass of 190.64 m/z. From second product ion by loss of $C_2H_3N$ with molecular mass of 149.59 m/z. From third product ion of 149.59 fourth product ion is formed due to the loss of $C_2HCl$ with the molecular mass of 91.12 m/z. Hence from all DP 3 was identified as 5-chloro-2-methyl-2,3,3a,12b-tetrahydro-1H-dibenzo[2,3:6,7]oxepino[4,5-c]pyrrole 2-oxide.

**DP 4 (m/z 255.35):**

DP 4 fragmentation pathway is shown in Figure 9 and mass spectrum shown in Figure 8 (D). In DP 4 parent ion fragment was observed at mass of 255.35 m/z. From that parent ion four product ions are formed. DP 4 product ions showed at 237.33 m/z, 161.24 m/z, 134.19 m/z, and 91.12 m/z. In addition, 237.33 m/z characteristic product ion formed due to the loss of $H_2O$ Oxidane (water). Alternately 161.24 m/z was formed from 237.33 m/z due to the loss of $C_6H_4$. From product ion of 161.24 m/z, 134.19 m/z third product ion was formed due to the loss of $C_2H_3$ (vinyl radical), and finally from this last by product ion was formed due to the loss of $C_2H_5N$ (ethanimine)

**Table 2.** LC–MS/MS data of DPs

| DP | Observed Mass | Formula | Calculated Mass | DB* | Major Fragments Along with Molecular Formula |
|---|---|---|---|---|---|
| DP 1 | 269.55 | $C_{16}H_{12}ClNO$ | 269.72 | 7 | 244.69 ($C_{14}H_{11}ClNO$), 192.62 ($C_{10}H_7ClNO$), 158.17 ($C_{10}H_8NO$), 101.12 ($C_8H_5$). |
| DP 2 | 287.34 | $C_{18}H_{22}ClN$ | 287.82 | 5 | 208.70 ($C_{12}H_{15}ClN$), 161.24 ($C_{11}H_{15}N$), 132.20 ($C_{10}H_{12}$). |
| DP 3 | 301.62 | $C_{17}H_{16}ClNO_2$ | 301.76 | 6 | 284.75 ($C_{17}H_{15}ClNO$), 190.64 ($C_{11}H_9ClN$), 149.59 ($C_9H_6Cl$), 91.12 ($C_7H_7$). |
| DP 4 | 255.11 | $C_{17}H_{21}NO$ | 255.35 | 5 | 237.33 ($C_{17}H_{19}N$), 161.24 ($C_{11}H_{15}N$), 134.19 ($C_9H_{12}N$), 91.12 ($C_7H_7$). |
| DP 5 | 253.27 | $C_{18}H_{23}N$ | 253.38 | 5 | 211.32 ($C_{16}H_{19}$), 158.23 ($C_{12}H_{14}$), 130.18 ($C_{10}H_{10}$), 93.14 ($C_7H_9$). |

* DB: Double bonds

with mass of 91.12 m/z. Finally, DP 4 was identified as 2-(1-methyl-4-phenylpyrrolidin-3-yl)cyclohexa-2,5-dien-1-ol.

**DP 5 (m/z 253.38):**

The fragmentation pathway of DP-5, shown in Figure 9, mass spectrum and further detailed in Figure 8 (E), indicates the DP 5 with molecular mass of m/z 253.38. Initial positive ESI LC-MS analysis yielded four fragments of DP-5 (m/z 211.32, 158.23, 130.18 and 93.14). First product ion from DP 5 is formed due to the loss of dimethylamine group ($C_2H_4N$) with mass of 211.32 m/z from parent ion, from first product ion another fragment was formed during the loss of 1,3-butadienyl radical ($C_4H_5$) with molecular mass of 158.23m/z. From second product ion by loss of ethylene group with molecular formula of $C_2H_4$ with molecular mass of 130.18 m/z. From third product ion of 130.18 fourth product ion is formed due to the loss of $C_3H$ with the molecular mass of 93.14 m/z. Hence from all DP 5 was identified as 3-(cyclohexa-1,3-dien-1-yl)-1-methyl-4-(6-methylidenecyclohexa-1,4-dien-1-yl)pyrrolidine.

## 3.2. Method Development and Validation

### *3.2.1 Method Development*

The study was commenced to propose quantitative analysis of asenapine along with its impurity 1 and 2. Additionally, the structural analysis of DPs was initiated in response to the stress encountered by asenapine, utilizing LC-MS/MS techniques. Firstly, HPLC method

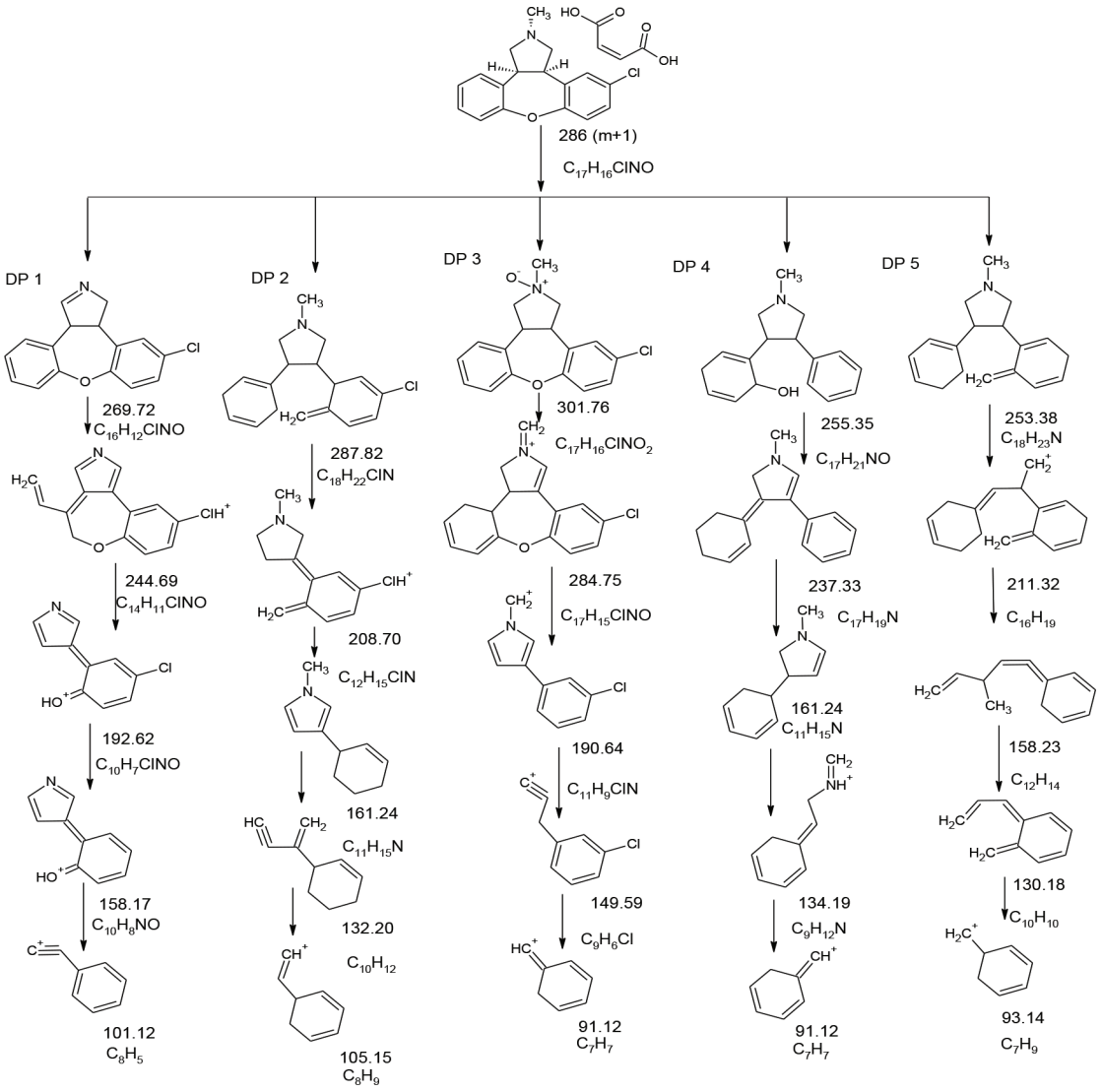



**Figure 9.** Fragmentation pathway of degradation products.

was optimised for the best results. Chromatographic parameters were optimized, including mobile phase composition, detection wavelength, and column, to enhance system efficiency. During method development, three distinct C18 analytical columns of 250 mm length such as BDS Y persil, YMC and kromasil were tested.

In optimization study, several factors such as tailing factor, retention time, and plate count were considered to find the best conditions for analysis. After examining these parameters, BDS Y persil C18 (250 mm) column was finalized for study. Next, different combinations of mobile phase compositions included a mixture of buffers, methanol, and orthophosphoric acid were tested. After careful evaluation, a mixture of 0.1% orthophosphoric acid, acetonitrile, and methanol in 50:30:20 (v/v) at 1.0 ml/min produced the well-resolved peaks and were detected at 231 nm wavelength. These conditions provided the best results for our analysis. Optimised conditions were given in Table 3.

**Table 3.** Optimized chromatographic conditions

| Parameter | Condition |
|---|---|
| Column Description | BDS Y Persil (250×4.6 mm; 5 µm id) C18 column |
| Sample Temperature | ambient |
| Wavelength | 231nm |
| Flow rate | 1.0 ml/min |
| Injection Volume | 20 µl |
| Run Time | 10 minutes |
| Mobile phase | 0.1 % Orthophosphoric acid, acetonitrile, and methanol in the ratio of 50:30:20 (v/v) |

### *3.2.2 Method Validation*

In order to ensure that system is working properly and can provide reliable results, a series of tests known as system suitability testing was conducted. For this, multiple samples of a standard solution containing asenapine at a concentration of 80 µg/ml was injected into system. During this testing, various parameters including the time it takes for the asenapine to appear (retention time), the size of peaks on chromatogram (peak area), the efficiency of separation process (plate count), the symmetry of peaks (tailing factor), and the degree of separation between neighbouring peaks (resolution) was measured. All of these measurements were recorded and analysed. The detailed results of our system suitability testing were then compiled and presented in Table 4 for easy reference and comparison. Additionally, a chromatogram in Figure 10, which shows how the system behaves when there are no sample components present (referred to as a blank chromatogram). Furthermore, Figure 11 illustrates the chromatogram obtained when the standard solution of asenapine is injected into the system, providing a visual representation of how the system performs under standard conditions. These analyses collectively ensure the reliability and robustness of our analytical system for subsequent sample analysis.

Linearity test was conducted to evaluate method effectiveness for analysing asenapine and its impurities. This involved examining change of peak area on chromatograms in relation to the concentration of asenapine and impurities. The results of our analysis indicated a linear relationship between the peak area and the concentration of asenapine across a concentration range from 20 to 140 µg/ml. Results achieved in this study were organized systematically in both Table 5

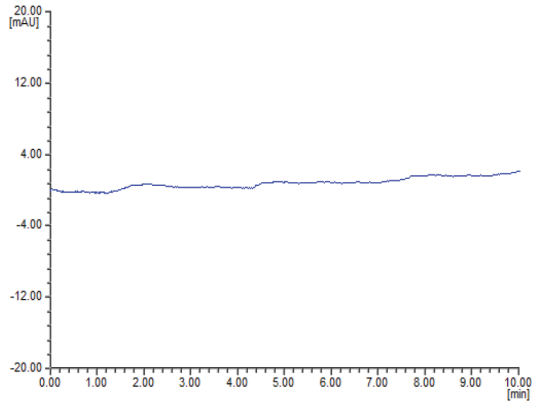



**Figure 10.** Blank chromatogram.

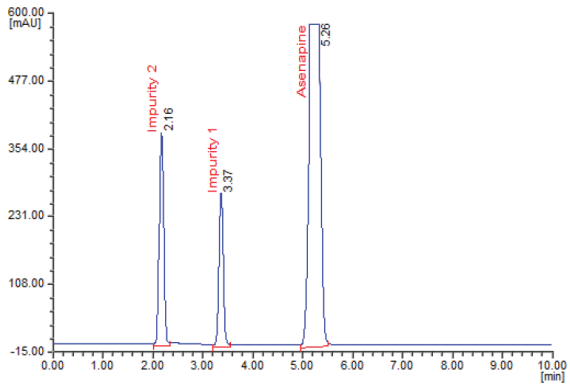



**Figure 11.** Standard chromatogram of asenapine.

and Table 6. Findings revealed a strong correlation between the peak area observed in our chromatograms and the concentration of asenapine within the specified concentration range. This suggests that method is reliable and capable of accurately quantifying the concentration of asenapine in samples across a wide range of concentrations.

**Table 4.** System suitability results

| Parameter | Asenapine | Value Impurities | Recommended Limits |
|---|---|---|---|
| Rt (min) | 5.26 | Imp 1 – 3.37<br>Imp 2 – 2.16 | --- |
| Area | 745409.5 (% RSD 1.09) | Imp 1 – 66990.1 (% RSD 0.77)<br>Imp 2 – 103872.8 (% RSD 1.10) | RSD ≤2 |
| Theoretical plate count | 9325 | Imp 1 – 5387<br>Imp 2 – 3518 | >2000 |
| Tailing factor | 0.99 | Imp 1 – 1.05<br>Imp 2 –1.01 | ≤2 |
| Resolution | 11.92 | Imp 1 – 4.88<br>Imp 2 – --- | --- |

The precision of the developed method was assessed through six replicate analyses of asenapine at a fixed concentration (80 µg/ml), yielding a % RSD of 0.25% for standard and 0.24, and 0.40 for impurities, affirming the intraday precision of the method. 0.31, 0.35, and 0.38 of % RSD for the asenapine and its impurities for interday precision. For ruggedness of asenapine and its impurities % RSD was found to be 0.49, 0.38, and 0.67. To verify the method's robustness, system suitability parameters were assessed under varying flow rates and column temperatures, focusing on retention time, tailing factor, and plate count. Analysis results (Table 7) revealed that minor alterations in method parameters had negligible effects on the analysis, confirming the method's robustness. To evaluate the method's accuracy, recovery studies were conducted at three concentrations (50%, 100%, and 150%) using the standard addition method (Table 8).

The developed HPLC method was utilized to measure impurities within a pharmaceutical asenapine formulation. The formulation sample was directly analyzed to assess impurity levels, and a formulation sample spiked with impurities was also analyzed to evaluate the method's ability to separate and quantify impurities. Chromatograms from the spiked formulation solution displayed distinct peaks corresponding to the studied impurities, confirming their identification. Conversely, chromatograms from the un-spiked formulation showed no peaks corresponding to the studied impurities, indicating impurity levels below the detection limit. This suggests that impurity levels in the sample were within permissible limits. Thus, the proposed method is deemed effective for quantifying impurities and DPs in asenapine.

**Table 5.** Linearity results of asenapine

| Concentration of Asenapine | Area Response | Concentration of Impurity | Area Response of Impurity 1 | Area Response of Impurity 2 |
|---|---|---|---|---|
| 20 | 287619.1 | 0.2 | 20524.2 | 31547.4 |
| 40 | 426157.3 | 0.4 | 35154.3 | 53374.2 |
| 60 | 582005.8 | 0.6 | 51219.3 | 79328.6 |
| 80 | 753627.5 | 0.8 | 67517.2 | 107483.4 |
| 100 | 916357.2 | 1 | 82321.4 | 131374.2 |
| 120 | 1052573.6 | 1.2 | 97658.7 | 158672.5 |
| 140 | 1212473.6 | 1.4 | 113254.1 | 186574.5 |

**Table 6.** Sensitive results

| Si No | Analyte | Asenapine | Results Noticed | |
|---|---|---|---|---|
| | | | Impurity 1 | Impurity 2 |
| 1 | Range (µg/mL) | 20-140 | 0.2-1.4 | 0.2-1.4 |
| 2 | a | 7788.8 | 77554 | 129951 |
| 3 | b | 124152 | 4764.1 | 2947.3 |
| 4 | $R^2$ | 0.9993 | 0.9999 | 0.9991 |
| 5 | LOD µg/mL | 0.60 | 0.06 | 0.06 |
| 6 | LOQ µg/mL | 2.0 | 0.2 | 0.2 |

**Table 7.** Ruggedness results in the proposed method

| S No | Altered condition | Analyte | % Estimated | % Change | Plate Count | Resolution |
|---|---|---|---|---|---|---|
| 1 | Detector wavelength as 236 nm | Asenapine | 1.08 | 98.92 | 9265 | 11.93 |
| 2 | | Impurity 1 | 0.29 | 99.71 | 5328 | 4.88 |
| 3 | | Impurity 2 | 0.84 | 99.16 | 3517 | --- |
| 4 | Detector wavelength as 226 nm | Asenapine | 0.23 | 99.77 | 9514 | 11.18 |
| 5 | | Impurity 1 | 0.62 | 99.38 | 5189 | 4.96 |
| 6 | | Impurity 2 | 0.26 | 99.74 | 3320 | --- |
| 7 | flow of 1.05 mL/min | Asenapine | 0.30 | 99.70 | 9103 | 11.54 |
| 8 | | Impurity 1 | 0.21 | 99.79 | 5377 | 4.36 |
| 9 | | Impurity 2 | 0.75 | 99.25 | 3487 | --- |
| 10 | flow of 0.95 mL/min | Asenapine | 0.63 | 99.37 | 9271 | 11.70 |
| 11 | | Impurity 1 | 0.73 | 99.27 | 5504 | 4.11 |
| 12 | | Impurity 2 | 0.73 | 99.27 | 3369 | --- |
| 13 | Mobile phase 50:40:10 (v/v) | Asenapine | 0.79 | 99.21 | 9455 | 11.58 |
| 14 | | Impurity 1 | 0.96 | 99.04 | 5691 | 4.61 |
| 15 | | Impurity 2 | 0.43 | 99.57 | 3503 | --- |
| 16 | Mobile phase 50:20:30 (v/v) | Asenapine | 0.21 | 99.79 | 9107 | 11.67 |
| 17 | | Impurity 1 | 0.93 | 99.07 | 5308 | 4.06 |
| 18 | | Impurity 2 | 0.85 | 99.15 | 3066 | --- |

**Table 8.** Accuracy results in the proposed method

| S No | Analyte | Level | Concentration (µg/mL) | | % Recovered | % RSD |
|---|---|---|---|---|---|---|
| | | | Prepared | Actual | | |
| 1 | Asenapine | 50 % | 60 | 59.300±0.43 | 98.83±0.727 | 0.74 |
| 2 | | 100 % | 80 | 79.445±0.653 | 99.31±0.817 | 0.82 |
| 3 | | 150 % | 100 | 99.383±0.616 | 99.38±0.616 | 0.62 |
| 4 | Impurity 1 | 50 % | 0.6 | 0.594±0.003 | 99.01±0.547 | 0.55 |
| 5 | | 100 % | 0.8 | 0.791±0.002 | 98.90±0.223 | 0.23 |
| 6 | | 150 % | 1.0 | 1.005±0.005 | 100.50±0.521 | 0.52 |
| 7 | Impurity 2 | 50 % | 0.6 | 0.596±0.005 | 99.41±0.887 | 0.89 |
| 8 | | 100 % | 0.8 | 0.796±0.011 | 99.46±1.358 | 1.37 |
| 9 | | 150 % | 1.0 | 0.997±0.010 | 99.70±1.100 | 1.10 |

The research looked at existing information and found that there wasn't any specific way mentioned in previous studies to measure asenapine and its impurities 1 and 2. Also, there wasn't any method reported to understand the DPs of asenapine. This means there's a gap in knowledge. So, this study aims to fill that gap by providing a method to measure asenapine and its impurities accurately, as well as a way to characterize its DPs. This study is important because it will help improve our understanding of asenapine and ensure better quality control in its production. One potential disadvantage of the proposed analytical approach lies in its complexity and resource-intensive nature. The integration of LC–MS techniques for the identification and characterization of DPs from asenapine demands specialized expertise and instrumentation, potentially limiting its accessibility to laboratories with comprehensive facilities and trained personnel.

## 4. Conclusion

This study focused on proposing a quantitative analysis method for asenapine and its impurities, along with initiating structural analysis of its DPs using LC-MS/MS techniques. The optimization process involved fine-tuning the HPLC method, including optimizing chromatographic parameters such as mobile phase composition, detection wavelength, and column selection. The BDS Y Persil C18 (250 mm) column and a mobile phase composition of 0.1% orthophosphoric acid, acetonitrile, and methanol in a ratio of 50:30:20 (v/v) at a flow rate of 1.0 ml/min were identified as the optimal conditions for analysis. System suitability testing confirmed the reliability and robustness of the analytical system, and linearity tests demonstrated a strong correlation between peak area and asenapine concentration. An elaborate forced degradation study was conducted on asenapine to assess its stability profile under a variety of stress conditions aimed at identifying its susceptibilities. The objective was to determine the conditions under which the drug exhibits labile characteristics. The outcomes of this comprehensive analysis showed that asenapine was sensitive to degradative changes when exposed to acidic, base and peroxide environments. Conversely, the drug displayed remarkable stability when subjected to UV and thermal stress. During the course of the LC separation experiments, it became apparent that five distinct DPs were produced as a result of the breakdown of different products. Among these, DP-1 emerged as a result of both acidic and basic conditions, whereas DP-4 was exclusively a consequence of the drug being exposed to acidic conditions. Additionally, two less prevalent degradants, DP-2 and 5 were identified as outcomes of acidic and base stress. While DP-3 was exclusively a consequence of the drug being exposed to peroxide conditions. To elucidate the molecular structures of these degradation products, a combination of MS, $MS^n$, and LC–MS/MS analytical techniques were employed. The data gathered from these analyses were instrumental in piecing together the comprehensive degradation pathway of asenapine.

## 5. Acknowledgements

Our gratitude to Department of Chemistry, Koneru Lakshmaiah Education Foundation, Vaddeswaram, Guntur for constant encouragement.

## 6. References

1. Shen WW. A history of antipsychotic drug development. Compr Psychiatry. 1999; 40(6):407-414. https://doi.org/10.1016/s0010-440x(99)90082-2
2. Aringhieri S, Carli M, Kolachalam S, Verdesca V, Cini E, Rossi M, *et al.* Molecular targets of atypical antipsychotics: From mechanism of action to clinical differences. Pharmacol Therapeut. 2018; 192:20-41. https://doi.org/10.1016/j.pharmthera.2018.06.012
3. Leucht S, Corves C, Arbter D, Engel RR, Li C, Davis JM. Second-generation versus first-generation antipsychotic drugs for schizophrenia: A meta-analysis. Lancet. 2009; 373(9657):31-41. https://doi.org/10.1016/s0140-6736(08)61764-x
4. Stacy P, Frantz J, Miller G, *et al.* A Narrative Review of the Pathophysiology and Treatment of Methamphetamine-Associated Psychosis. Int J Ment Health Addiction. 2024. https://doi.org/10.1007/s11469-024-01323-y
5. Bhupatiraju RV, Kasimala BB, Nagamalla L, Sayed F. Structural evaluation of degradation products of loteprednol using LC-MS/MS: Development of an HPLC method for analyzing process-related impurities of loteprednol. Anal Sci Technol. 2024; 37 (2): 98-113.
6. Bhupatiraju RV, Kumar BS, Tangeti VS, Kandula R, Sayed F. LC and LC-MS/MS studies for identification and characterisation of related substances and degradation products of abrocitinib. Toxicol Int. 2024; 31(2): 321-334. https://doi.org/10.18311/ti/2024/v31i2/36370
7. Auclair J, Rathore AS. Analytical methods to determine the stability of biopharmaceutical products. LCGC N Am. 2023; 41(1):23–27. https://doi.org/10.56530/lcgc.na.qc1477t9
8. Varma RB, Rao BS. Gas chromatography-head space-flame ionization sensor based assessment of four residuary solvents in rivaroxaban bulk medication. Res J Pharm Technol. 2022; 15(11):5158-5163. https://doi.org/10.52711/0974-360x.2022.00868
9. Bhupatiraju RV, Battula SR, Kapavarapu MVNR, Mandapati VR. Assessment of gas chromatography methodology approach for the trace evaluation of carcinogenic impurity. methyl chloride, in trimetazidine dihydrochloride. Ann Pharm Fr. 2023; 81(1):64-73. https://doi.org/10.1016/j.pharma.2022.06.012
10. Fagiolini A, Forgione RN, Morana B, Maccari M, Goracci A, Bossini L, *et al.* Asenapine for the treatment of manic and mixed episodes associated with bipolar I disorder: From clinical research to clinical practice. Expert Opin Pharmacother. 2013; 14(4):489-504.11. https://doi.org/10.1517/14656566.2013.765859
11. Shahid M, Walker GB, Zorn SH, Wong EH. Asenapine: A novel psychopharmacologic agent with a unique human

receptor signature. J Psychopharmacol. 2009; 23(1):65–73. https://doi.org/10.1177/0269881107082944
12. Meltzer HY, Dritselis A, Yasothan U, Kirkpatrick P. Asenapine. Nat Rev Drug Discov. 2009; 8:843–844. https://doi.org/10.1038/nrd3027
13. Govindarajan N, Koulagari S, Methuku A, Podhuturi S, Venkata RB. Method development and validation of RP-HPLC method for determination of new antipsychotic agent asenapine maleate in bulk and in pharmaceutical formulation. Der Pharmacia Lettre. 2012; 4(6):1805-1810.
14. Chhalotiya UK, Bhatt KK, Shah DA, Patel JR. Stability-indicating liquid chromatographic method for the quantification of the new antipsychotic agent asenapine in bulk and in pharmaceutical formulation. Sci Pharm. 2012; 80(2):407–417. https://doi.org/10.3797/scipharm.1112-07
15. Pansuriya K, Shelat P, Patel H. Development and validation of RP-HPLC method for quantitative determination and estimation of asenapine maleate in bulk and buccal (effervescent) dosage form. Int J Pharm Sci Rev Res. 2020; 2317-2323. https://doi.org/10.13040/IJPSR.0975-8232.11(5).2317-23
16. Patel K, Joshi D, Kumbhani J, Prajapati V. HPLC method development for estimation of dissolution of antipsychotic drug as sublingual film dosage form. Chem Sci Trans. 2018; 7(3):420-423. https://doi.org/10.7598/cst2018.1495
17. Patel PS, Patel CN, Patel MM. Analytical method development and validation of RP-HPLC for estimation of asenapine maleate in bulk drug and tablet dosage form. Int J Pharm Res. 2016; 5(4):15-19.
18. Aarelly K, Thimmaraju MK, Nerella R, Allabotharam S. Method development and validation of asenapine in bulk by RP-HPLC method. J Chem Pharm Res. 2012; 45: 2580-2584.
19. Kalpana GL, Devalarao G, Raju MB, Praveenkumar T. Validated stability indicating high performance liquid chromatographic method for the quantification of asenapine maleate. Int J Pharm Sci. 2015; 7(11):61-65.
20. Shyamala, Swarupa A, Anitha P. Validated stability-indicating RP-HPLC method for determination of asenapine. Indo Am j pharm sci. 2018; 05(05):4107-4113.
21. Borkar AA, Gaikwad NJ. UV spectrophotometric and RP-HPLC estimation of drug asenapine in tablet dosage form. Int J Pharm Sci Res. 2016; 7(7):3080-3084. https://doi.org/10.13040/IJPSR.0975-8232.7(7).3080-84
22. Al-Nimry SS, Khanfar MS. Validation of an RP-HPLC method for the determination of asenapine maleate in dissolution media and application to study *in vitro* release from co-crystals. Sci Pharm. 2021; 89(1):14. https://doi.org/10.3390/scipharm89010014
23. Managuli RS, Kumar L, Chonkar AD, Shirodkar RK, Lewis S, Koteshwara KB, *et al.* Development and validation of a stability-indicating RP-HPLC method by a statistical optimization process for the quantification of asenapine maleate in lipidic nano formulations. J Chromatogr Sci. 2016; 54(8):290-1300. https://doi.org/10.1093/chromsci/bmw062
24. Kovatsi L, Titopoulou A, Tsakalof A, Samanidou V. HPLC analysis of antipsychotic asenapine in alternative biomatrices: Hair and nail clippings. J Liq Chromatogr Relat Technol. 2015; 38(18):1666-1670. https://doi.org/10.1080/10826076.2015.1089894
25. Reddy AVB, Venugopal N, Madhavi G. Simultaneous determination of asenapine and valproic acid in human plasma using LC–MS/MS: Application of the method to support pharmacokinetic study. J Pharm Anal. 2013; 3(6):394-401. https://doi.org/10.1016/j.jpha.2013.04.008
26. Patel NP, Sanyal M, Sharma N, Patel DS, Shrivastav PS, Patel BN. Determination of asenapine in presence of its inactive metabolites in human plasma by LC-MS/MS. J Pharm Anal. 2018; 8(5):341-347. https://doi.org/10.1016/j.jpha.2018.06.002
27. De Boer T, Meulman E, Meijering H, Wieling J, Dogterom P, Lass H, *et al.* Quantification of asenapine and three metabolites in human plasma using liquid chromatography–tandem mass spectrometry with automated solid-phase extraction: Application to a phase I clinical trial with asenapine in healthy male subjects. Biomed Chromatogr. 2012; 26(2):156-165. https://doi.org/10.1002/bmc.1640
28. ICH Q2(R1) Guideline: Validation of analytical procedures: Text and methodology. International Conference on Harmonization (ICH), IFPMA; 2005.
29. Bhupatiraju RV, Kumar BS, Peddi P, Tangeti VS. An effective HPLC method for evaluation of process related impurities of letermovir and LC-MS/MS characterization of forced degradation compounds. J Chem Metrol. 2023; 17(2):181-198. https://doi.org/10.25135/jcm.98.2311.2975
30. Varma BHR, Rao BS. Gas chromatography-head space-mass spectrometry sensor based quality control of dobutamine hydrochloride bulk material for a mutagenic impurity, 2-bromopropane. Res J Chem Environ. 2023; 27(2):54-61. https://doi.org/10.25303/2702rjce054061
31. Varma RB, Battula SR, Kapavarapu MVNR, Mandapati VR. A novel rivaroxaban degradation impurity detection by RP-HPLC extraction by preparative chromatography, and characterization by LC-MS, NMR and FT-IR: Analysis of novel impurity in batch samples and tablets of rivaroxaban. Rasayan J Chem. 2022; 15(4):2373-2381. https://doi.org/10.31788/rjc.2022.1547008
32. Raju PMK, Shyamala P, Narayana BV, Dantuluri HSNR, Bhupatiraju RV. A fast, validated UPLC method coupled with PDA-QDa detectors for impurity profiling in betamethasone acetate and betamethasone phosphate injectable suspension and isolation, identification, characterization of two thermal impurities. Ann Pharm Fr. 2022; 80(6):837-852. https://doi.org/10.1016/j.pharma.2022.03.003